

# Sample Manuscript

of

## 14<sup>th</sup> International Conference on Recent Advances in Concrete Technology and Sustainability Issues October 30 – November 2, 2018 Beijing, P.R. CHINA

### **ORGANIZED BY:**

*The Chinese Ceramic Society*  
*Committee for the Organization of*  
*International Conferences*  
*(Formerly CANMET/ACI Conferences)*

### **SPONSORED BY:**

*China Academy of Building Research*

### **CO-SPONSORED BY**

*American Concrete Institute(U.S.A.)*  
*Institute of Concrete Technology (U.K.)*  
*Sinoma Research Institute*  
*Technical Committee of Concrete*  
*Admixture Application Technology*  
*Technical Committee of Concrete Quality*  
*Chinese Concrete Admixture Association*  
*Beijing University of Technology*  
*Tsinghua University*  
*Southeast University*

**October 30 – November 2, 2018**  
**Beijing, CHINA**

Website: <http://www.hpcsp.org>

### **Conference Honorary Chairpersons**

V. Mohan Malhotra  
Changwen Miao

### **Conference Chairperson**

Yongmo Xu

### **ORGANIZING COMMITTEE**

#### **Director**

Zhanping Jin  
The Chinese Ceramic Society  
Qingqin Wang  
China Academy of Building Research

### **SCIENTIFIC COMMITTEE**

#### **Chairpersons**

Tongbo Sui  
Sinoma Research Institute,  
Johann Plank  
Technische Universität München

### **SECRETARIAT**

#### **General Secretary**

Ziming Wang  
Beijing University of Technology

#### **Secretary-Treasurer**

Jingyu Guo  
China Academy of Building Research

## **FROM HPC TO HPSS: NEW FRONTIERS IN WASTE STABILIZATION**

Giorgio Ferrari, Nodar Al-Manasir, Gilberto Artioli, Silvia Contessi, Roberto Pellay, Loris Calgaro

### **Biography:**

**Giorgio Ferrari** graduated in Chemistry at Padua University (Italy) in 1977 and presently is senior researcher in Mapei for concrete admixtures and development of sustainable concrete technologies. He is author of several scientific publications and international patents on concrete technology and of two books on environmental issues

**Nodar Al- Manasir** is Research and Development Manager for concrete admixtures at Mapei AS, Norway. She received her PhD from Department of Chemistry, University of Oslo, Norway. Her recent interest is improvement and development of concrete admixtures.

**Gilberto Artioli** graduated at the University of Modena (Italy) and received his PhD in Geophysical Sciences from the University of Chicago. He is presently full Professor at the University of Padua (Italy) and Director of the CIRCe Centre for the investigation of cement materials.

**Silvia Contessi** graduated in Environmental Sciences at Padua University in 2017 and she is presently performing her PhD at Geoscience department of Padua University

**Roberto Pellay** is CEO of Intec, a company specialized in waste and wastewater treatment processes, located in Malcontenta di Mira, Venice (Italy).

**Loris Calgaro** graduated in Chemistry at the University of Venice (Italy) in 2016 and he is presently performing his PhD at the Venice University.

## **ABSTRACT**

Solidification/Stabilization (S/S) of waste with cement is one of the most common technique to reduce the mobility of inorganic contaminants of waste materials. Heavy metals are precipitated in the calcium rich alkaline environment and can be intercalated in the newly formed hydrated cement phases. The present paper describes a new process which applies the principles of High Performance Concrete (HPC) to the S/S process, by using PCEs superplasticizer in order to reduce the mixing water and the capillary porosity of the stabilized materials. The new High Performance S/S process (HPSS) transforms the waste into a cementitious granular material characterized by high mechanical properties and low leaching of contaminants. The new stabilized granular material can be easily implemented with additional treatments to further improve its environmental compatibility and mechanical performance. Removal of volatile and semi-volatile organic contaminants from the granular material can be accomplished by vacuum distillation at relatively high temperature (lower than 250 °C) without deteriorating the cement microstructure

**Keywords:** contaminants, leaching, porosity, solidification-stabilization, superplasticizers, waste

## **INTRODUCTION**

Stabilization/Solidification (S/S) technology aims at decreasing mobility and toxicity of inorganic contaminants (stabilization) by encapsulating the material into a solid with structural integrity (solidification) and includes a wide range of processes, most of them based on inorganic binders such as Portland cement (Cullinane et al. 1986). This treatment is increasingly used in situ or ex situ for the remediation of contaminated soils; for instance, 24 per cent of the US Superfund program

remedial actions involving source-control in the period 1982-2002 were based on S/S technologies (US EPA 2004). However, concerns over the long-term performance of S/S materials have been raised due to the degradation of the cement structure over the time.

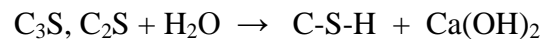
This paper presents an improved process for the treatment of contaminated soil and sediments, both by inorganics and organics, based on the principles of High Performance Concrete (HPC), which substantially improve the characteristics of the cement matrix of S/S materials. This process has been implemented with an additional step to remove the volatile and semi-volatile organic compounds from the solidified materials.

## **THE PRINCIPLES OF HIGH PERFORMANCE CONCRETE**

The American Concrete Institute (ACI) defines High Performance Concretes as concretes meeting special combinations of performance and uniformity requirements which cannot be achieved routinely when using conventional constituents and normal mixing, placing and curing practices. One of the commentary to the definition states that a high-performance concrete is one in which certain characteristics are developed for a particular application and environment. Examples of characteristics which are considered critical in HPC are: long term mechanical properties, permeability, density, volume stability and long life in severe environment. All these properties are related and depend on the amount of water used in the concrete mixture. In fact, it is well known that water to cement ratio (W/C) is the main factor which determines most of the properties of hardened concrete; by lowering W/C, also the porosity of the microstructure of the cement paste and consequently its permeability to liquid and gaseous aggressive agents from the environment are reduced and all the aforementioned properties are consequently improved.

Superplasticizers are essential ingredients for the production of HPC; they consist of water soluble polyelectrolytes which dramatically reduce the viscosity of fresh cement mixtures and allow to cast flowable, easy to place concretes characterized by low W/C ( $\leq 0.4$ ). Modern superplasticizers are based on synthetic polymers derived from the copolymerization of acrylic acid and polyetheracrylates. These new polymers are characterized by higher efficiency and better environmental compatibility in comparison with the previous generation of superplasticizers, based on polycondensates of naphthalene sulfonate and formaldehyde. They act by means of complex mechanisms of adsorption, electrosteric stabilization, deflocculation and dispersion of cement grains in the fresh concrete mixture and are used at dosages ranging from 0.6 to 1.5 per cent according to the type of cement and the design of the concrete (Collepari and Valente 2006).

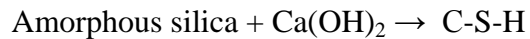
Other important ingredients for the production of HPC are mineral admixtures, such as natural pozzolana, silica fume, fly-ash and other pozzolanic materials. The hydration of the silicate phases of Portland cement produces calcium silicate hydrates and calcium hydroxide (portlandite) according to the following reaction:



where  $C_3S = 3CaO \cdot SiO_2$ ,  $C_2S = 2CaO \cdot SiO_2$  and C-S-H represents calcium silicate hydrates.

Portlandite crystals, due to their high solubility (about 2 mg/L) can be dissolved by the water present in the pores and washed off from the cement microstructure. This process causes the progressive broadening of the capillary pores and favours the intrusion of aggressive agents from the environment (sulphates, chlorides) which accelerate the degradation of concrete microstructure.

Pozzolanic materials are added to cement mixtures at dosages from 5 to 30 per cent and react with calcium hydroxide present in cement mixtures forming additional silicate hydrates, according to the following reaction:



This reaction produces the double beneficial effect of transforming the highly soluble portlandite in the less soluble C-S-H and reducing the porosity of cement microstructure by the formation of new silicate hydrated products. The combination of superplasticizers and mineral admixtures presently represents the best way to improve the microstructure of cement paste and consequently to produce High Performance Concrete with improved durability (Collepari 2006).

## **THE IMPROVED S/S PROCESS**

The principles of HPC have been applied in an improved S/S process (Mapei HPSS – High Performance Solidification Stabilization) based on the use of superplasticizers and a specific production plant to produce, starting from contaminated soils and sediments, artificial cement aggregates characterized by improved environmental compatibility, mechanical strength and durability in comparison with similar aggregates produced without such additives.

The process is effective on finely divided materials. Therefore, after excavation it is necessary to preliminary treat the contaminated soil or sediment to remove both the waste materials larger than 2 mm and the excess of water, in order to leave a residual humidity content of about 15-20 %; this result can be obtained both by filter-press and/or by air drying directly on site; a few percent of CaO can be useful to speed up this drying step.

The pre-treated soil or sediment is then mixed with cement, the superplasticizer and in an intensive mixer. The resulting mixture is a wet, finely divided mass, with the same aspect of the starting soil/sediment, but due to the intensive mixing and the effect of the superplasticizer, micro-seeds of aggregates are formed inside the whole mass. This mixture is then transferred to a rotating plate where the micro-seeds can grow up to the desired dimension, with the addition of few percent of water, if required. The rotating plate of an industrial plant is shown in Figure 1.



Figure 1. Rotating plate apparatus used for the pelletization process of the aggregates. Diameter of the plate: ~ 3.5 m.

The final dimension of the grains depends on the speed of rotation, the inclination of the plate and the residence time. A typical particle size distribution of the final granular materials ranges from 4 mm to 16 mm, with no fractions lower than 2 mm. Once they are formed, the granular materials are cured at normal conditions and, after hardening, can be reused at the jobsite for filling or other

applications. Figure 2 shows the appearance of the aggregates obtained with the S/S process described in the present paper.



Figure 2. Artificial granular aggregates obtained with the proposed S/S process. The diameter of the largest grains is approximately 16 mm.

With this improved method it is possible to produce dense, homogeneous artificial aggregates from contaminated soil and sediments, characterized by an extremely low amount of mixing water. In fact, by using the superplasticizers and the wet granulation process, it is possible to produce granular material characterized by a water to solid ratio (W/S) of 0.20 or less, where the term “solid” is referred to the sum of soil and cement.

This process has been developed for the treatment of soil and sediments characterized by inorganic contamination (mainly heavy metals); in the case of organic contamination, the process can be integrated with a distillation step. The granular materials produced in the first step are heated in a reactor at 200 - 250 °C at reduced pressure ( $P < 0.1$  bar), in order to distillate the organic



contaminants from the grains. By this way, it is possible to remove more than 95 % of volatile and semi-volatile organic contaminants (light and heavy hydrocarbons, dioxins, PCBs, PAHs). Furthermore, due to the mild operating conditions, the cement microstructure of the grains is not substantially degraded and the mechanical properties of the granular materials remain essentially the same.

In the present work, the efficiency of the proposed S/S process has been evaluated with a soil contaminated by heavy metal collected in an industrial area close to the city of Venice (Italy). Due to the inorganic characteristics of the contamination, only the first granulation step of the process has been applied in the present work.

## **EXPERIMENTAL**

### **Samples description**

All the samples studied in this work were prepared using the contaminated soil coming from the "ex-Conterie" industrial site in Murano (Venice, Italy). This area represents the first example (currently operating) of an industrial-scale application of the presented S/S process for the requalification of a contaminated site. Until 1990, this was the site of a factory for the manufacture of artistic glass which introduced a significant environmental contamination, mainly due to inorganic pigments and adjuvants based on heavy metals and arsenic. Approximately 30000 m<sup>3</sup> of soil are estimated to have been involved in the contamination. The mean values of concentration for the main contaminants in the soil are reported in Table 1.

Table 1. Mean contamination of the “ex-Conterrie” soil.

Contaminant	Unit	Concentration
Arsenic (As)	mg/kg dw	204
Cadmium (Cd)	mg/kg dw	11.9
Chromium (Cr)	mg/kg dw	55.1
Copper (Cu)	mg/kg dw	279
Mercury (Hg)	mg/kg dw	1.84
Lead (Pb)	mg/kg dw	2321

The concentration of As, Cd, Cu, Hg and Pb exceeded the Italian regulatory limits of soils for residential destination, with As and Pb exceeding also the limits for industrial destination.

Two distinct sets of granular samples have been produced with the soil and then investigated here. The grains included in the first batch (Sample A) were prepared with the wet granulation step without superplasticizer, while those belonging to the second group (Sample B) were produced following the presented process, using the Mapeplast ECO1, a PCE superplasticizer produced by Mapei, based on copolymer of methacrylic acid and methoxypolyethyleneglycol methacrylate, with EO side chains of MW = 1000 dalton.

The composition of the different samples is reported in Table 2.

Table 2. Composition of the different samples tested.

Ingredient/Property	Composition (g)	
	Sample A	Sample B
“Ex-Conterie” soil	1000	1000
Type I Portland cement	400	400
Mapeplast ECO1	-	11
H <sub>2</sub> O	280	210
W/S <sup>(*)</sup>	0.20	0.15

<sup>(\*)</sup> W/S = Water to solid ratio (sum of soil and cement).

From Table 2 it can be seen that Sample A, produced by the wet granulation process without superplasticizer, required 25 % more water in comparison with Sample B, produced with a dosage of 0.8 % of additive by weight of the whole solid material.

Both sets of samples were cured for more than 60 days in normal conditions (23 °C and 95 % r.h.) before being subjected to X-ray computed micro-tomography, mercury intrusion porosimetry, leaching tests and physico-mechanical tests.

## **X-ray computed micro-tomography**

X-ray computed micro-tomography (X- $\mu$ CT) is an established technique for the three-dimensional (3D) microstructural investigation of many kind of materials. It represents an evolution of the CT-scan method, originally developed for medical purposes. At present, X- $\mu$ CT has found application in several research fields including geology, materials science, archaeology, engineering and biomedicine, using both conventional (microfocus) scanners and synchrotron-based systems. During the last decade, X- $\mu$ CT has been successfully applied also to the characterization of cement-based materials (e.g. Bentz et al. 2000, Helfen et al. 2005, Burlion et al. 2006, Gallucci et al. 2007). Besides the access to the third dimension, one of the major advantages of X- $\mu$ CT comes from its total non-invasiveness, as no prior preparation of the sample is required. As it is well known, in cement-based materials, the specimen preparation procedure (e.g. for optical or electronic microscopy analyses) may introduce problematic artifacts. Although the spatial resolution level offered by scanning electron microscopy has not been reached yet, even by the most performing synchrotron-based systems, X- $\mu$ CT represents an invaluable tool for the extraction of qualitative and quantitative data from cement pastes, mortars and concretes.

A typical experimental setup for micro-tomography consists of three components: an X-ray source, a rotating sample holder and a digital detector. During the data collection, a series of co-planar radiographic projections (up to several thousands) is acquired with the sample being rotated relative to the source-detector pair by small angular steps. Once all the two-dimensional radiographs are collected, a reconstruction algorithm, as for example Filtered Back-Projection (Kak and Slaney 1988), can be applied to produce a stack of cross-sectional images called slices, each one representing what would be seen if the object was physically cut along a plane normal to its rotation axis. Each reconstructed slice is actually a matrix of voxels (volume elements in a 3D digital image) whose gray values (GV) are proportional to the mean X-ray attenuation coefficient within the

corresponding volume of material (dark for low- and bright for high-attenuating features). The well known Beer-Lambert's law relates the variation between the incident and the detected beam intensity to the linear attenuation coefficients ( $\mu$ ) of the materials and to the length of the X-ray path through them. For every single material,  $\mu$  is related to its electron density, its mean atomic number and to the energy of the beam.

Tomographic scans on the S/S products were carried out at the Tomolab facility, Basovizza (Trieste), Italy. Tomolab is a custom-made, cone-beam micro-CT system, equipped with a sealed, polychromatic microfocus X-ray tube (*Hamamatsu L9181S*) with micrometric focal spot size. This x-ray source can operate at a maximum voltage and current of 130 kV and 300  $\mu$ A respectively; the target material (anode) is tungsten. X-ray radiographic images are collected by an high-resolution CCD camera (*Photonic Science X-ray Imager VHR*, 4008x2670 pixels) characterized by a large field of view and a small pixel size. A tapered bundle of optical fibers, connects the CCD plate to a gadolinium oxysulphide (GadOx) scintillator screen, with a resulting active area for acquisition of approximately 50x33 mm<sup>2</sup> and a pixel size of 12.5  $\mu$ m. The scintillator is optimized for the detection of X-ray energies in the range of 20-85 keV, roughly corresponding to the region of maximum photon flux in the emission spectrum of the source. The movement of the sample is ensured by two translational stages (along vertical and lateral directions) and a rotation stage (around the vertical axis) controlled by high-precision electrical motors. As for other micro-CT systems, the spatial resolution achievable depends on the sample dimensions, the focal spot size, the technical characteristics of the CCD and, due to the cone-beam geometry, the magnification factor (M). This parameter, which is the ratio between the source-detector distance and the source-object distance, can be adjusted by manually translating the sample holder and/or the CCD along a rail.

The microtomography experiments described here were mainly focused on the investigation of the microstructure of the pore system that plays a fundamental role in cement-based materials not only

for their mechanical properties but also for their durability (e.g. freeze-thaw resistance) and transport properties. A few samples, approximately 6-8 mm in diameter, were selected from the two groups (sample A and B) of solidified grains; the chosen size was a good compromise between representativeness, overall X-ray absorption and spatial resolution achievable. The source voltage and the beam current were slightly adjusted for each experiment according to the amount of absorption shown by the sample and varied in the range of 70-74 kV and 108-110  $\mu$ A. 1440 projections over a 360° rotation (angular step: 0.25°) were acquired per each scan, with an exposure time per frame ranging from 5000 to 5300 ms. The source-object and source-detector distances were set at 80 and 330 mm respectively ( $M = 4.125$ ). With this experimental setup, the voxel size in the final image was approximately 6  $\mu$ m. A 0.5 mm thick aluminum filter was placed in front of the source in order to suppress the lower energies of the spectrum and reduce the beam hardening effect. This latter is a common artifact in microfocus tomography, related to the preferential attenuation of the lower energy X-rays as they travel through the sample. In the final reconstructed slices, this results in the central portion of the image appearing to be less attenuating than the outer parts. During data collections, the CCD detector operated in 2x2 binning mode, i.e. the signal is averaged on four adjacent pixels that work as a single superpixel. This of course reduces the resolution of the images but the signal to noise ratio can be significantly improved. The reconstruction of the slices from the acquired 2D projections was carried out using the Feldkamp-Davis-Kress (FDK) algorithm (Feldkamp et al. 1984) implemented in the Cobra software package (Exxim Computing Corporation). A beam hardening correction based on a polynomial fitting was also applied during the reconstruction process. Ring artifacts, caused by anomalous responses from some elements of the detector, were successfully removed from the reconstructed slices using the filter developed by Brun et al. (2009) starting from the approach proposed by Sijbers and Postnov (2004). This procedure gave excellent results, strongly improving the quality of the images and

allowing the extraction of quantitative information. After reconstruction, each entire original data sets, composed by more than 1000 contiguous slices, was down-sampled from a 16-bit to a 8-bit gray scale, in order to reduce the file sizes and the computational times for the analyses. The contrast of the reconstructed images was then enhanced by stretching the GV histograms of the stacks, trying to keep brightness and contrast as constant as possible between different samples. A gentle smoothing of the images was then performed by using a 3x3x3 median filter that allowed to reduce the noise without significantly modifying the information contained in the data sets. For each sample, the pore fraction was then extracted by accurately thresholding the reconstructed images on the basis of their gray value histograms, thus obtaining a stack of binary images where voids are represented in black ( $GV = 0$ ) and the solid fraction in white ( $GV = 255$ ). It should be pointed out that significant errors may be introduced during this step, so particular care has to be taken in the choice of the threshold value, especially when comparisons between different samples have to be made. For each sample, almost the entire reconstructed volume has been considered for the calculations of the porosity, excluding only the upper and lower slices of the stack. In order to work with a larger, more representative volume, no cropping of the central portion of the slices was performed; this was possible because the edge effects due to beam-hardening could be reasonably neglected here. After the segmentation of the pore fraction, the total entrained air content and the pore size distribution were calculated. All the image processing operations described here were carried out using the Image J software (Abramoff et al. 2004) and related plugins.

### **Mercury intrusion porosimetry**

Mercury intrusion porosimetry (MIP) is a widely used technique for the characterization of the pore space properties of many materials, including cement-based materials. It can provide indirect measurements of total porosity, pore size distribution and other related properties, detecting pores

ranging from a few hundreds of  $\mu\text{m}$  down to the nm scale. In the present study, MIP experiments have been carried out in order to estimate the differences in total porosity and pore size distribution between S/S grains produced by the wet process without additives (Sample A) and those prepared using superplasticizers (Sample B). MIP is based on the fact that mercury is a non-wetting fluid, so a pressure needs to be applied in order to force the liquid metal into the empty pores of a certain material. By progressively incrementing the pressure applied to the mercury surrounding the sample, increasingly smaller pores can be intruded. The well-known Washburn's equation (3) relates the diameter of the intruded pore to the applied pressure, in a porous system assumed to be constituted of a network of cylindrical pores, entirely and equally connected to the exterior of the sample. Washburn's equation is usually written as follows:

$$d = -4g\cos\theta/P$$

where  $d$  is the diameter of the cylindrical pore being intruded,  $g$  is the surface tension of mercury ( $\sim 0.48 \text{ N/m}$  at  $20^\circ\text{C}$  under vacuum),  $\theta$  is the contact angle between mercury and the solid (typically between  $135^\circ$  and  $142^\circ$ ) and  $P$  is the applied pressure.

MIP measurements have been carried out at the Environmental Agronomy Department of the University of Padua (Italy) using two Thermo Scientific Pascal 140/240 porosimeters. The first instrument can reach an intrusion pressure of 0.4 MPa, detecting pores ranging from  $\sim 200$  to  $\sim 4 \mu\text{m}$  in diameter while the second one can measure the finer pore fraction (diameter up to 6-8 nm) with a maximum pressure of 200 MPa. For each measurement, in order to improve the statistical significance of the experiment, several S/S grains (previously dried) were put inside the porosimetry chamber at the same time, for a total mass of approximately 4 grams of material.



### **Leaching tests**

Leaching tests were conducted on fractions of granular materials of Sample A and Sample B, according to the EN 12457/2 method. 100 grams of each sample, after reduction of the grain size below 4 mm, were mixed with 1 liter of deionized water (liquid to solid ratio L/S = 10) for 24 hours. Eluates from the leaching tests were analyzed according to the EPA 6020A method by the ICP-MS technique (Perkin-Elmer ICP-MS spectrometer, mod. ELAN DRC).

### **Thermal analysis**

The thermogravimetric technique was used to evaluate the presence and the amount of portlandite originated from the hydration of cement in the artificial aggregate produced with the presented method. Analyses were performed by using a STA409 (Netzsch) Thermo Gravimetric Analysis/Differential Scanning Calorimeter (TGA/DSC) on 40-50 mg of specimen, with an heating ramp rate of 40 °C/min (from 20 to 1100 °C) in static air.

### **Physico-mechanical tests**

The physico-mechanical properties of the artificial cement-based granular materials, both with and without superplasticizer, were measured according to the standard methods normally used for aggregates. Specific gravity and water absorption were measured according to the UNI-EN1097-6:02 method. Resistance to fragmentation was measured with two different methods: ACV, according to BS-812-100 and Los Angeles test, according to UNI-EN1097-2. Freeze-thaw resistance was measured according to UNI-EN1367-1 and alkali-silica reactivity was evaluated by UNI8520/22:02.

## RESULTS AND DISCUSSION

### X-ray computed micro-tomography

The stacking of all the reconstructed X- $\mu$ CT slices allowed the internal structure of the investigated samples to be visualized in 3D, as shown in Figure 3.

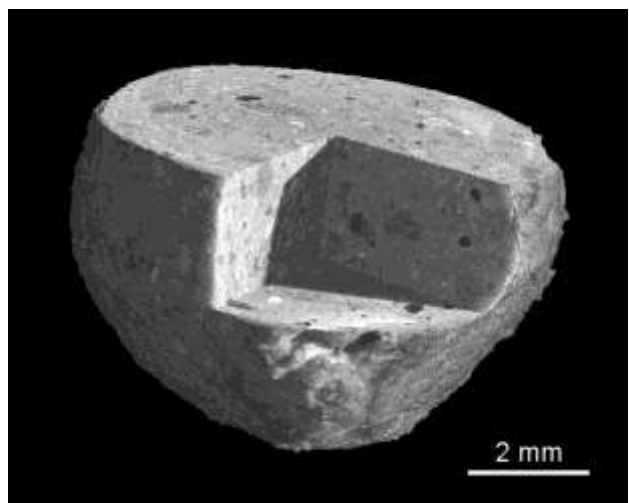


Figure 3. 3D reconstruction of a cement-based S/S grain prepared according to the presented method. A portion of the whole dataset has been digitally removed in order to visualize the interior of the sample. Darker gray values correspond to low attenuation (mostly air voids) and brighter ones to high-absorbing particles (metals, lead-containing glass).

Several distinct features were clearly recognized in the reconstructed images as for example entrained air bubbles, heterogeneous mineral grains, glass fragments, vegetal remains, mollusc shells and several very highly absorbing particles of probable metallic nature. All these elements were of course contained in the original contaminated soil, some of them naturally included, others

introduced by the glass production activity formerly operating in the “ex-Conterie” site. The mentioned presence of dense, highly attenuating particles was a problematic issue during the image analysis procedure. In fact, if these particles are large enough to cause the incoming X-ray beam to be completely stopped, severe artifacts can be introduced into the reconstructed slices. These are generally seen as black shadows and streaks around the high-absorbing particles, creating a region characterized by a total lack of information that may be mistakenly considered as a void. This problem could be partially overcome by increasing the energy of the beam but this would of course cause a loss of contrast in all the other portions of the image. Therefore, in some cases, a manual correction was necessary to correct such artefacts, in order to avoid an overestimation of the entrained air content.

Figure 4 shows a comparison between two reconstructed slices obtained from two S/S grains prepared without and with superplasticizer. By looking at the two images, a significant difference in total air void content as well as in void shape and size can be clearly recognized. The total entrained air content, calculated (over the entire 3D volume) after the segmentation of the pore fraction by simply dividing the number of black voxels by the total number of voxels (solids and voids) is 5.17 % for the conventional S/S grain (Sample A) and 1.97 % for the sample prepared using superplasticizers (Sample B). It should be pointed out that the size of a considerable amount of pores in cement-based materials is well below the resolution level of the technique (voxel size ~ 6  $\mu\text{m}$  in this specific case), thus making their discrimination from the solid matrix practically impossible. Hence, our investigation was limited to larger, isolated (at least at this spatial resolution) air voids with a diameter greater than 10  $\mu\text{m}$ . It should also be noted that some low-attenuating organic particles may show very low gray values in the reconstructed images, so they can be hardly discriminated from pores just by thresholding the GV histogram. The volume of each individual pore was calculated using the Object Counter 3D plugin of ImageJ and their size was

then approximated according to the equivalent sphere diameter (i.e. the diameter of the sphere having the same volume as that pore). Significant differences were found between the two series of samples as illustrated by the histograms of pore size distribution of Figure 5. Even without taking into account the few very large ( $> 500 \mu\text{m}$ ) air voids, the pores contained in the conventional S/S grain result to be distributed over a broader range of sizes if compared to the sample prepared using additives. Moving from the conventional sample to that produced with the superplasticizer, the relative amount of pores whose equivalent diameter is smaller than  $100 \mu\text{m}$  increases from 21.7 % to 39.9 %. Moreover, in the first case, the maximum peak of the distribution corresponds to the 100-120  $\mu\text{m}$  class while in the second one the dominant interval is 60-80  $\mu\text{m}$ . The comparison of the reconstructed slices of Figure 4 and the results of Figure 5 clearly confirm that the use of a superplasticizer in the wet S/S granulation of the “Ex-Conterie” contaminated soil significantly reduced the entrained air content (pore sizes from 10  $\mu\text{m}$  to 400  $\mu\text{m}$ ) of the final product. This is a direct effect of the reduction in the viscosity of the soil-water-cement fresh mix, induced by superplasticizers.

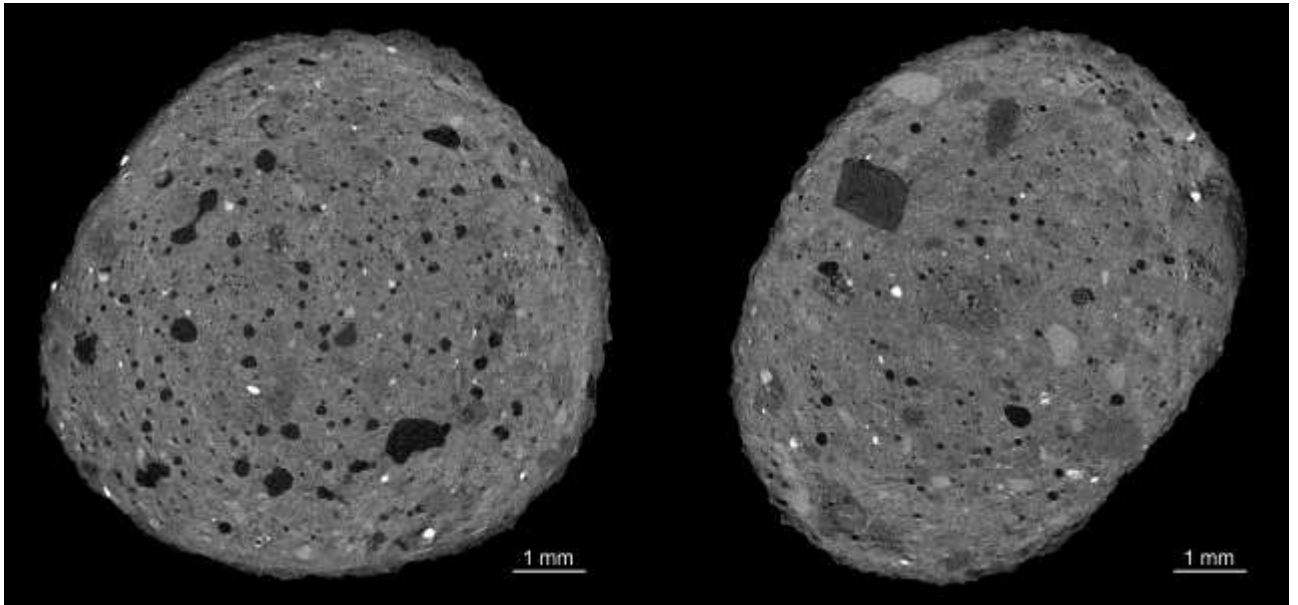


Figure 4. Cross-sectional reconstructed slices illustrating two S/S grains prepared without (left) and with (right) additives. A more compact matrix, with a significantly lower air void content can be achieved following the S/S procedure presented here.

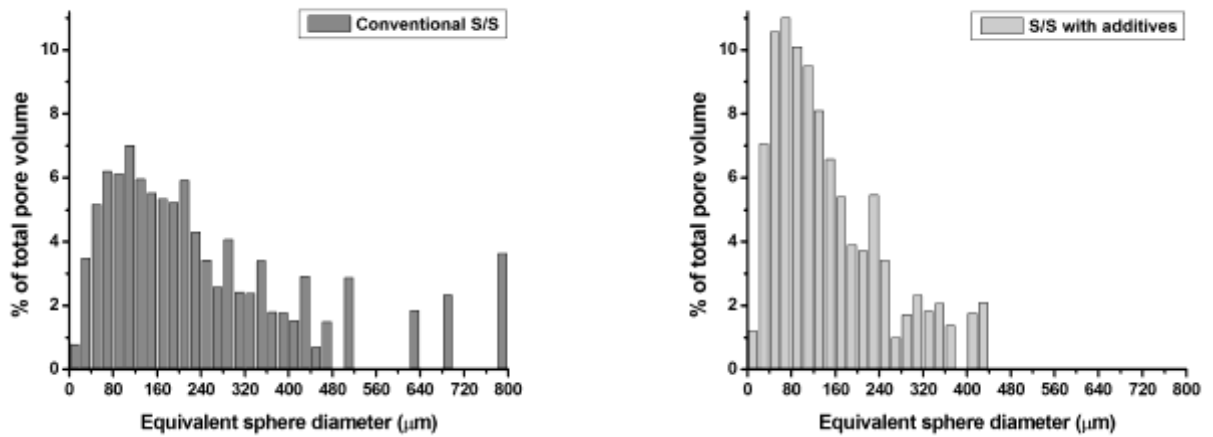


Figure 5. Pore size distribution histograms calculated from the analysis of tomographic data for two S/S grains formulated without (left) and with (right) superplasticizers. The relative fraction of the total pore volume was plotted versus the equivalent sphere diameter. The bin

width is 20  $\mu\text{m}$ . Due to limitations in the spatial resolution of the technique, pores smaller than 10  $\mu\text{m}$  were not detectable, so they were not included in the calculations.

### Mercury intrusion porosimetry

In Figure 6 a comparison between two porosimetric curves of the granular materials obtained without (solid line) and with superplasticizer (dashed line) is reported.

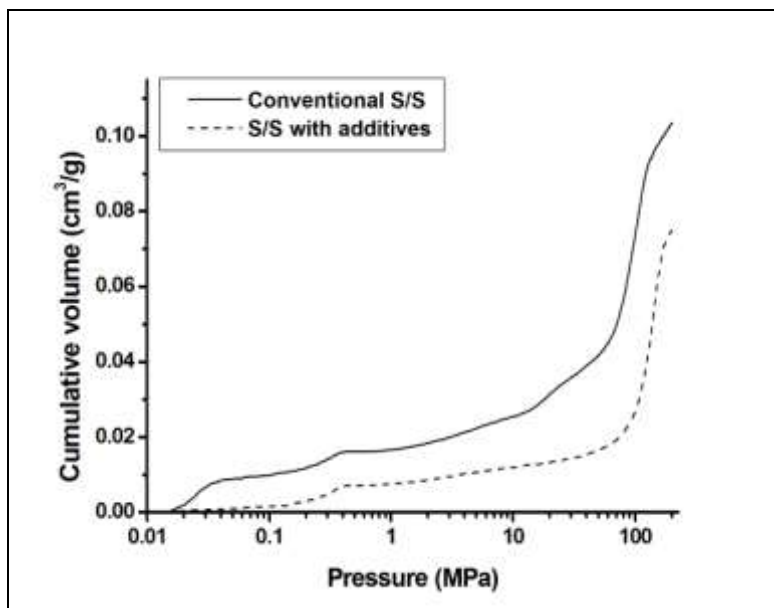


Figure 6. Porosimetry curves obtained for S/S grains prepared with (dashed line) and without (solid line) superplasticizer. The cumulative volume of mercury intruded per gram of sample was plotted versus the applied pressure.

As a first result, it can be easily seen that the curve referring to the samples with the superplasticizer lies below the curve measured for the conventional S/S grains, clearly indicating a reduced total connected porosity. In particular, the measured total void content decreases from 20.07 % to 15.34 % of the entire sample volume. In this graph, the minimum and maximum data points of the curves roughly correspond to intruded pores having diameters of 100  $\mu\text{m}$  and 6 nm respectively. A slight change in the slope of the two curves at

0.4 MPa of intruding pressure is indeed an artifact due to the non-perfectly smoothed connection between the data points measured with the first and the second porosimeter. The use of superplasticizers seems to be effective in reducing porosity both at the larger and the thinner pore level. During the very early stages of intrusion (up to 0.04 MPa) a significantly larger volume of mercury is intruded in the conventional S/S sample if compared to the additivated one, as confirmed by the different slopes of the two curves. This indicates that the coarser pore fraction ranging approximately from 100 to 40  $\mu\text{m}$  (as calculated from pressure values) is far more represented in the first sample. From that point, the two datasets assume a nearly parallel trend until 5-6 MPa (roughly corresponding to a pore diameter of 0.4  $\mu\text{m}$ ), where the upper curve starts increasing again its slope. A remarkable change in the lower curve is seen only at very high pressure values thus indicating that the great majority of porosity is concentrated in the dimensional interval below 15-20 nm. This evidences seem to confirm that a lower W/C ratio and the use of superplasticizers substantially contribute to the reduction of micrometer and sub-micrometer scale porosity, creating a more dense matrix. According to many authors, pores larger than 50 to 100 nm may be detrimental to strength and permeability of cement paste (Metha 1986 and Goto and Roy 1981). Therefore, the observed decrease of the porosity in the sub-micrometer scale of the granular material produced with the superplasticizer are expected to produce improvement of the environmental and mechanical properties of the artificial aggregates.

For what concerns the differences between the two samples in the low-pressure (high diameter) part of the graph, a major role may be played by the region commonly referred to as the interfacial transition zone (ITZ). In concretes and mortars, ITZ is a thin, heterogeneous region of paste existing between the cementitious matrix and the surface of the aggregate particles, characterized by increased porosity and concentration of portlandite crystals if

compared to the matrix paste (see for example Bonen 1994, Scrivener and Nematı 1996, Shane et al. 2000). In our specific case, the aggregates are represented by the grains included in the contaminated soil that was used for the preparation of the S/S products. Though there is no complete agreement about the mechanisms of formation, ITZs are likely to form as a result of an inefficient packing of cement grains at the aggregate surface (Ollivier et al. 1995). The relevant amount of coarser porosity (left part of the graph) detected in conventional S/S samples is probably related to the presence of a percolating network of pores originating from contiguous ITZs around the aggregate grains. Superplasticizers, coupled with a lower W/C ratio of the mix, are thought to inhibit the growth of ITZs, thus hampering the formation of a preferential pathway for the percolation of fluids. This is demonstrated by the very low amount of mercury intrudable during the initial, low-pressure stages for the additivated samples.

For the interpretation of pore size distributions in the region of the micropores (right part of the graph), extreme care has to be taken when dealing with cement-based samples. In fact, in this kind of materials, the pore system usually does not satisfy the requirements of the classical model, thus giving rise to problematic artifacts in the output data. For example, as shown by electron microscope investigations, the shape of the pores in an hydrated cement paste is far more complex than the ideal network of cylindrical tubes of the classical Washburn's model. Anyway, this can be considered a minor problem, affecting to different extents also many other materials. A major issue is related to the fact that the great majority of the pores are not directly linked to the outer surface and can be reached by mercury only after it has traveled through a long and complex series of intermediate pores of different sizes and shapes (Diamond 2000). A critical role is played by the presence inside cement pastes, mortars and concretes of a significant fraction of relatively large entrained air voids, as



shown also in the present work by means of X- $\mu$ CT. It is widely accepted that these air bubbles are not isolated but are part of the percolating pore system. In practice, a large air void inside the matrix cannot be reached by mercury until a certain threshold pressure value is reached, necessary to fill the smaller channels that lead to the said void. At that point, the large pore starts to act as a reservoir for mercury and the corresponding intruded volume is mistakenly referred to the threshold pressure and hence attributed to a much finer pore fraction which will then result overestimated. This phenomenon is commonly referred to as the “ink-bottle effect”. Due to these intrinsic limitations related to the microstructure of cement-based materials, some authors (e.g. Diamond 2000) suggested that MIP should not be considered a completely reliable method for the determination of the pore size distribution and other associated parameters. However, this technique still remains an invaluable tool for the determination of the total intrudable volume enabling to detect pores having sizes several orders of magnitude smaller than those measurable with other techniques, as for example X- $\mu$ CT.

### **Leaching tests**

The concentration of heavy metals in the eluates of the “Ex-Conterie” soil exceeded the regulatory standard of the Italian Government for the reusable materials (Decree of Ministry of the Environment n. 186/2006) for Arsenic (As), Chromium (Cr), Copper (Cu) and Lead (Pb), as shown in Table 3. The eluates of the aggregate produced without the superplasticizer (Sample A) complied with the standards for all the metals except for Copper; this metal, most at the high values of pH typical of Portland cement mixtures, forms complexes with soil soluble organic matter and therefore increases its solubility (Xue and Sigg 1999). On the other side, Sample B, produced by the wet granulation with the superplasticizer, complied

with the regulatory limit for all the contaminants.

Table 3. Comparison of leaching values of the different contaminants for the “Ex-Conterie” soil and the aggregates produced without superplasticizer (Sample A) and with superplasticizer (Sample B).

Analyte	Unit	Concentration			
		Soil	Sample A	Sample B	Regulatory Limits
As	µg/L	1254	7	<1	50
Cd	µg/L	3.9	<0.1	<0.1	5
Cr	µg/L	64	<1	<1	50
Cu	µg/L	175	100	20	50
Hg	µg/L	<0.1	<0.1	<0.1	1
Pb	µg/L	218	25	10	50

These results confirm the importance of using superplasticizers in S/S processes, in order to improve the environmental compatibility of the solidified products.

### **Thermal analysis**

The graph of Figure 7 shows the thermogravimetric analysis of a sample of an artificial aggregate produced from the “Ex-Conterie” soil with the improved S/S method. It is important to note that there is no detectable loss of weight at the temperature of about 500 °C, corresponding to the transition:

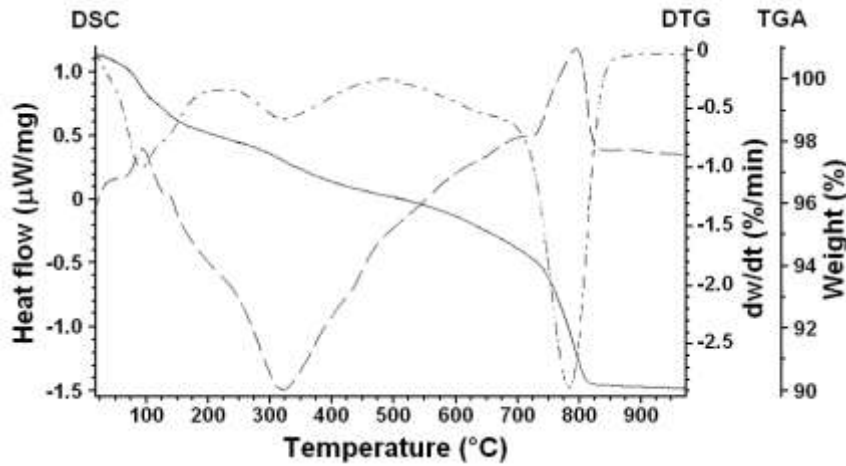
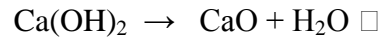


Figure 7. Thermogravimetric analysis (TGA, solid line), differential thermal gravimetry (DTG, dash-dotted line) and differential scanning calorimetry (DSC, dashed line) curves of an artificial aggregate produced with the improved S/S process. No significant loss of weight is detectable at ~500 °C, the dissociation temperature of portlandite.

These results seem to indicate that portlandite produced by cement hydration reacts with some components present in the soil, through a pozzolanic-like reactions. Similar results were obtained by treating a marine sediment using S/S technology (Ferrari et al. 2000).

### Physico-mechanical tests

The results of the physical and mechanical tests performed on the granular materials without and with the superplasticizer (Sample A and B, respectively) are shown in Table 4.

Table 4. Physical and mechanical properties of artificial aggregates produced without (Sample A) and with superplasticizer (Sample B).

Parameter/Property	Unit	Sample A	Sample B
Specific gravity	Mg/m <sup>3</sup>	2.17	2.33
Water absorption	%	6.6	2.5
ACV	%	29	24
Los Angeles	%	42	35
Freeze/Thawing	%	5.5	3.2
Alkali/Silica reaction	-	negative	negative

Results of Table 4 indicate that all the physical and mechanical properties of the artificial aggregate produced with the presented S/S process are definitely improved by the addition of the superplasticizer. As a result of the reduction of porosity of the granular material produced with the superplasticizer, also the freeze-thaw resistance is improved and consequently the durability of the resulting material.

## CONCLUSIONS

Superplasticizers are essential components for the production of High Performance Concrete. Their importance lies in their capability to reduce the amount of mixing water and, consequently, to improve all the physico-mechanical properties (strength, permeability) and the durability of concrete.

The results of the present study indicate that superplasticizers can be successfully applied also in S/S technology to reduce the leaching of contaminants of stabilized soils and sediments. These results are obtained through the reduction of the porosity over a broad range of pores, from coarser to finer pores (below 100 nm), as confirmed by X-ray tomography and mercury intrusion porosimetry analyses.

The reduction of the mixing water improves all the physical and mechanical properties of the granular materials prepared with the S/S technology. Also the durability of the cement-based granular materials produced from the contaminated soil is improved, both for the reduction of the porosity and for pozzolanic reactions with the soil mineralogical matrix.

However, further investigations are necessary in order to assess the possibility to reuse the artificial aggregates produced with the proposed S/S process as filling materials, aggregates for concrete and for other civil engineering projects.

## REFERENCES

- Abramoff, M.D., Magelhaes, P.J. and Ram, S.J. 2004. Image processing with ImageJ, *Biophotonics International*, 11(7): 36-42.
- Bentz, D.P., Quenard, D.A., Kunzel, H.M., Baruchel, J., Peyrin, F., Martys, N.S. and Garboczi, E.J. 2000. Microstructure and transport properties of porous building materials. II: Three-dimensional X-ray tomographic studies, *Materials and Structures*, 33(3): 147-153.
- Bonen, D. 1994. Calcium hydroxide deposition in the near interfacial zone in plain concrete, *Journal of the American Ceramic Society*, 77: 193-196.
- Brun, F., Kourousias, G., Dreossi, D. and Mancini, L. 2009. An improved method for ring

- artifacts removing in reconstructed tomographic images, *World Congress on Medical Physics and Biomedical Engineering, IFMBE Proceedings*, Munich (Germany), 25: 926-929.
- Burlion, N., Bernard, D. and Chen, D. 2006. X-ray microtomography: application to microstructure analysis of a cementitious material during leaching process, *Cement and Concrete Research*, 36(2): 346-357.
- Colleparidi, M. 2006. *The New Concrete*, ENCO, Ponzano Veneto, Italy.
- Colleparidi, M. and Valente M. 2006. Recent Developments in Superplasticizers, 8<sup>th</sup> *CANMET/ACI International Conference on Superplasticizers and Other Chemical Admixtures in Concrete*, ACI SP-239, Sorrento, Italy, 1-14.
- Cullinane, M.J., Jones, L.W., and Malone P.G. 1986. *Handbook for Stabilization/Solidification of Hazardous Waste*, EPA/540/2-86/001, U.S. Environmental Protection Agency, Cincinnati, OH, USA.
- Diamond, S. 2000. Mercury porosimetry: an inappropriate method for the measurement of pore size distributions in cement-based materials, *Cement and Concrete Research*, 30: 1517-1525.
- Feldkamp, L.A., Davis, L.C. and Kress, J.W. 1984. Practical cone-beam algorithm, *Journal of the Optical Society of America*, A1(6): 612-619.
- Ferrari, G., Cerulli, T., Clemente, P., Pistolesi, C., Salvioni, D. and Surico, F. 2000. Durability of High-Performance Mortars Containing Contaminated Marine Sediments in Aggressive Environments, 5<sup>th</sup> *CANMET/ACI International Conference on Durability of Concrete*, ACI SP-192, Barcelona, Spain, 659-675.
- Gallucci, E., Scrivener, K., Groso, A., Stampanoni, M. and Margaritondo, G. 2007. 3D experimental investigation of the microstructure of cement pastes using synchrotron X-ray

- microtomography ( $\mu$ CT), *Cement and Concrete Research*, 37: 360-368.
- Goto, S. and Roy, D. 1981. Diffusion of Ions through Hardened Cement Pastes. *Cement and Concrete Research*, 11: 751-757.
- Helfen, L., Dehn, F., Mikulik, P. and Baumbach, T. 2005. Three-dimensional imaging of cement microstructure evolution during hydration. *Advances in Cement Research*, 17(3): 103-111.
- Kak, A.C. and Slaney, M. 1988. *Principles of Computerized Tomographic Imaging*, IEEE Press, New York, NY, USA.
- Metha, P.K. 1986. *Concrete: Its Structure, Properties and Materials*, Prentice-Hall, Englewood Cliffs, NJ.
- Ollivier, J.P., Maso, J.C. and Bourdette, B. 1995. Interfacial transition zone in concrete. *Advanced Cement Based Materials*, 2(1): 30-38.
- Scrivener, K.L. and Nematy, K.M. (1996). The percolation of pore space in the cement paste/aggregate interfacial zone of concrete, *Cement and Concrete Research*, 26(1): 35-40.
- Shane, J.D., Mason, T.O., Jennings, H.M., Garboczi, E.J. and Bentz, D.P. (2000) Effects of the interfacial transition zone on the conductivity of Portland cement mortars. *Journal of the American Ceramic Society*, 83: 1137-1144.
- Sijbers, J. and Postnov, A. 2004. Reduction of ring artifacts in high resolution micro-CT reconstructions, *Physics in Medicine and Biology*, 49: N247-N253.
- U.S. EPA 2004. *Treatment Technologies for Site Cleanup: Annual Status Report* (Eleventh Edition), EPA-542-R-03-009.
- Xue, H. and Sigg, L. 1999. Comparison of the Complexation of Cu and Cd by Humic or Fulvic Acids and by Ligands Observed in Lake Waters. *Aquatic Geochemistry*, 5: 313-335.